Progress In Electromagnetics Research, Vol. 133, 555–570, 2013

COMPACT AND HIGH ISOLATION MICROSTRIP DIPLEXER FOR BROADBAND AND WLAN APPLICATION

H. W. Deng*, Y. J. Zhao, Y. Fu, J. Ding, and X. J. Zhou

College of Electronic and Information Engineering, Nanjing University of Aeronautics and Astronautics, Nanjing 210016, China

Abstract—In this paper, a compact and high isolation microstrip diplexer is designed for broadband and wireless local area network (WLAN) application, simultaneously. The bandpass filter (BPF) for broadband channel is formed by three-coupled-line structure and two short stubs with different size loaded in 50 Ω feed lines, and the BPF for WLAN channel consists of two coupling quarter-wavelength resonators (QWR) and one open stub loaded in short parallel-coupling feed structure. Multiple transmission zeros can be generated due to their intrinsic characteristics, so the broadband BPF with sharp skirt and wide upper-stopband performance and the WLAN BPF with sharp roll-off and lower-stopband characteristic can be realized. The tapped stub not only can generate new transmission zeros to deepen the stopband, but also can connect other BPF as an its part without deterioration of in-band performance. Hence, a compact microstrip diplexer combines of two BPFs without the extra junction matching network. The mutual loading effect approximately equivalent to a coupled QWR can also generate new transmission zero at the passband edge to improve the isolation. A microstrip diplexer with the 3 dB fractional bandwidths (FBW) of 80% for broadband channel and 5% for WLAN channel is designed and fabricated. Good agreement between the simulated and measured results is observed.

1. INTRODUCTION

A diplexer, as an essential component in multi-service and multi-band communication systems, is a three-terminal device which lets two or more frequencies into one input port and then separating them to two

Received 23 September 2012, Accepted 5 November 2012, Scheduled 8 November 2012

* Corresponding author: Hong Wei Deng (hwdeng@nuaa.edu.cn).

other output ports. A well designed diplexer should have low cost and high performance. Microstrip diplexers as low cost ones can be easily mounted on the dielectric substrate and can provide a more flexible design of the circuit layout [1]. Hence, microstrip diplexers were widely studied in the early 1960s by Matthaei et al. [2] and Wenzel [3]. In the past few years, much effort on the microstrip diplexer has been paid to reduce the size and improve the performance. Due to the interaction of two filters composing the diplexer, the characteristics of a microstrip diplexer are different from the responses of the individual two microstrip filters. The complexity of the interaction makes the design of a microstrip diplexer complicated [4].

For the design of microstrip diplexers, the traditional approach is to design the two different filters individually and then to design a matching circuit. The most intuitive approach is to combine two BPFs with a T-junction or Y-junction [5–10]. The method, which features the filter A (filter B) an open-circuit-load shunted to the filter B (filter A) at the frequency of the latter, is adopted to figure the dimensions of the connecting line for reducing the mutual loading effect between the filters. Owing to the well development of the BPF implementation [11, 12], it is relatively easy to design decent diplexers based on this approach. This kind of diplexers, however, usually occupies a considerable footprint due to the required large size from the junction. In [13–16], the common resonator technology is proposed to remove the input junction in the diplexer designs and reduces the size to a large degree. However, since the passbands of the diplexer rely on the first two resonant frequencies of the common resonator, the common resonator needs to be chosen properly. Some interesting diplexer designs without distribution networks have appeared in the recent literatures [17–21]. A new topology of the diplexer with the common port directly connected to two filters was proposed and synthesized in [17], although no design example was given. A design procedure for coupled resonator diplexers that does not employ any external junctions was also reported in [18], and was further verified in [19]. In addition, the composite right/left-handed transmission lines [20] and substrate integrated waveguide (SIW) with complementary split-ring resonators [21] can be applied to the diplexer designs, which do not require matching network. Despite compact diplexers can be obtained, isolation and insertion loss of these diplexers are not satisfactory.

Furthermore, broadband or ultra-wideband (UWB) modern commination systems [22–25] have promoted the development of the microstrip diplexer with broadband channel. But there are few literatures until now concerning microstrip diplexer with broadband

or UWB application. In a previous work [26], a microstrip diplexer for Bluetooth and UWB application is presented by combining two ring-like BPFs with tapped T-junction coupling line. A UWB microstrip diplexer in [27] is formed by two hairpin line filtering structures without the matching network and a tapped open stub used to introduce an attenuation pole to suppress the spurious response. However, the above mentioned diplexers [26, 27] in fact have the drawbacks such as low isolation and large dimension.

In this paper, a compact and high isolation microstrip diplexer for broadband and WLAN [28, 29] application is designed through the combination of two BPFs without the extra junction matching network. The BPF for broadband channel is formed by three-coupled-line structure and two short stubs with different size loaded in 50 Ω feed lines, and the BPF for WLAN channel consists of two coupling QWRs and one open stub loaded in short parallel-coupling feed structure. Multiple transmission zeros can be created to achieve high out-band rejection of two filters owing to their intrinsic characteristics. The tapped stub connects other high out-band rejection BPF as an its part without deterioration of in-band performance. Because of the coupling between the tapped stub and the QWR, new transmission zero can be created at the other channel passband edge to improve the isolation. Finally, a microstrip diplexer is designed and fabricated, and a satisfactory agreement between the simulated and measured results validates the proposed configuration.

2. HIGH ISOLATION MICROSTRIP DIPLEXER DESIGN

2.1. Analysis of the Uniform Resonator Coupling Tapped Stub

As well-known, the stub loaded in the 50 Ω feed lines can be applied to generate new transmission zeros. And the transmission zeros generated by the open stub and short stub can be expressed as, respectively:

$$f_{open} = nc/\left(4\sqrt{\varepsilon_e}\, l\right); \quad f_{short} = nc/\left(2\sqrt{\varepsilon_e}\, l\right), \tag{1}$$

where l refers to the length of the stub, c the speed of light, and ε_e the equivalent dielectric constant.

Furthermore, the effects of the coupled different end uniform resonators on the open and short tapped stubs are investigated. The current distributions of six different cases are simulated by HFSS and shown in Figure 1. The substrate used is RT/Duroid 5880 with a thickness of 0.508 mm, permittivity of 2.2 and loss tangent 0.0009. We can directly see that only the currents of the short uniform resonator

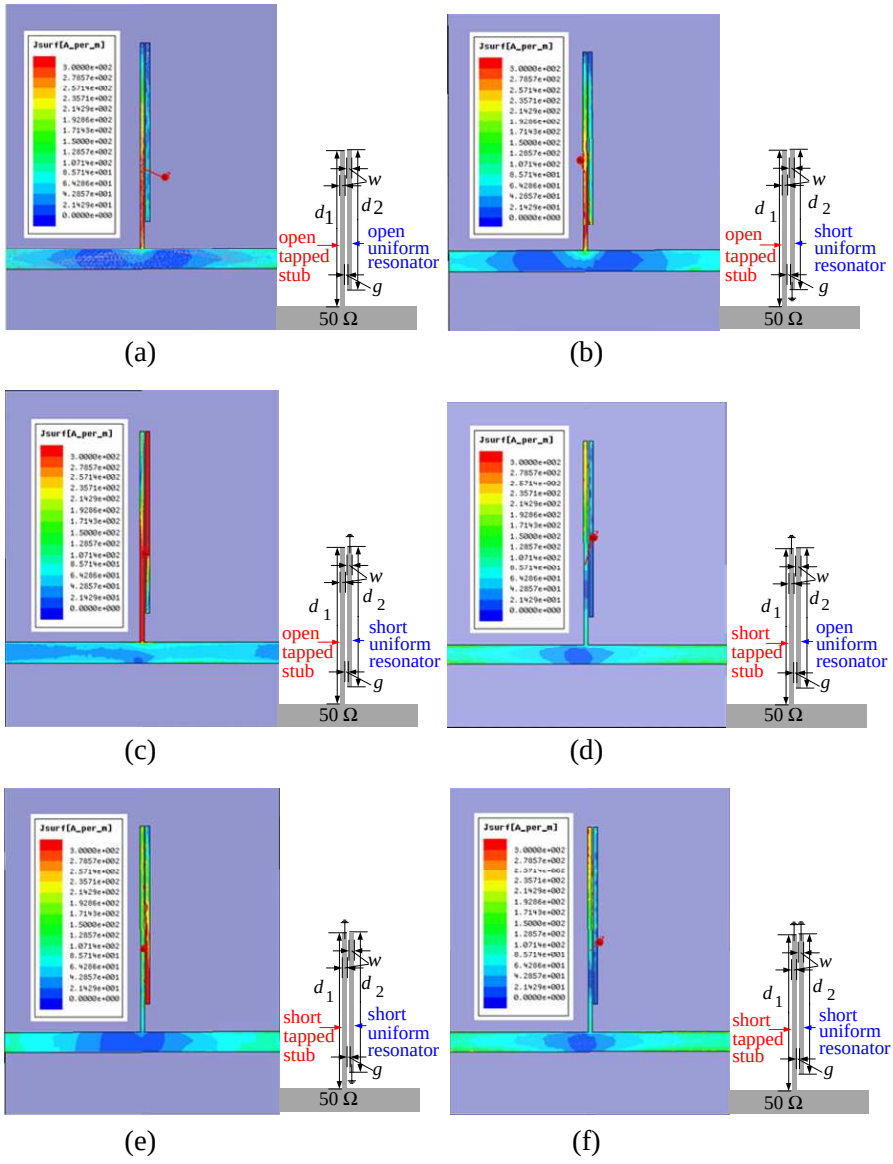

Figure 1. Current distributions at 5 GHz of the different end uniform resonator coupling open and short tapped stubs. (The structural parameters are: $d_1 = 15$ mm; $d_2 = 13$ mm; $w = 0.3$ mm; $g = 0.1$ mm).

in Figures 1(c) and (e) are very strong distribution, but the current distribution in Figure 1(c) is strongest.

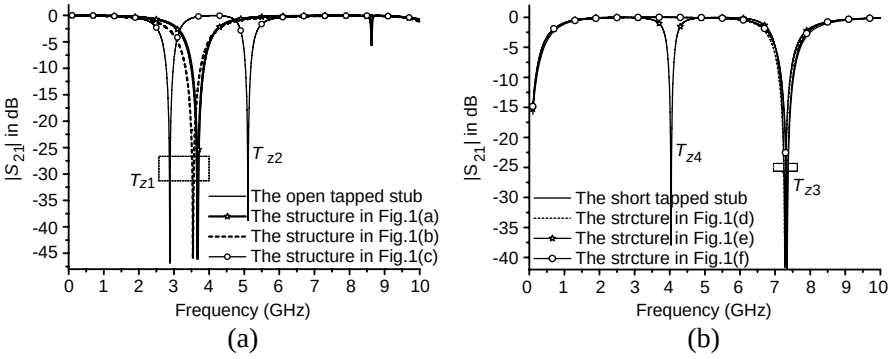

Figure 2. The $|S_{21}|$ in dB of the different end uniform resonator coupling tapped stubs. (a) Open tapped stub. (b) Short tapped stub.

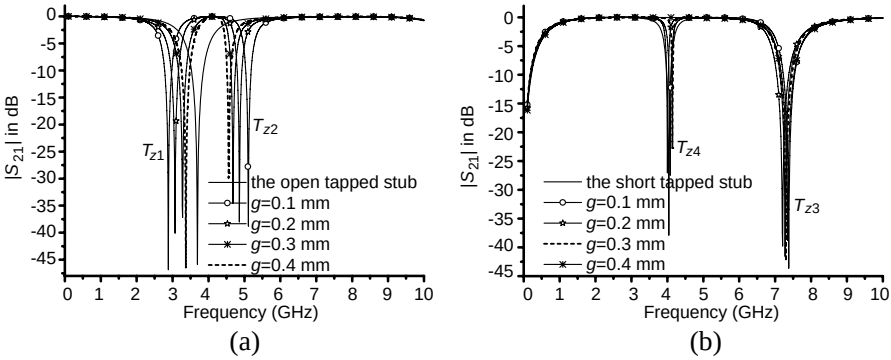

Figure 3. The simulated $|S_{21}|$ in dB with varied g. (a) The coupling open tapped stubs in Figure 1(c). (b) The coupling short tapped stubs in Figure 1(e).

The $|S_{21}|$ in dB of the different end uniform resonator coupling tapped stubs in the range of 0.1–10 GHz are interpreted in Figure 2. The uniform resonators in the structures in Figures 1(a), (b), (d) and (f) have less effect on the first transmission zero created by the tapped stub and cannot generate new transmission zero, for the mutual coupling between the uniform resonator and the tapped stub is very weak. But the short uniform resonators in the structures in Figures 1(c) and (e) can generate new transmission zeros T_{z2} and T_{z4}, respectively. As the gap g decreased, the transmission zero T_{z2} approximately equal to $c/(4\sqrt{\varepsilon_e}d_2)$ GHz moves towards upper frequency, as shown in Figure 3(a), whereas the transmission zero T_{z1} created by the open tapped stub moves downwards. We can see that

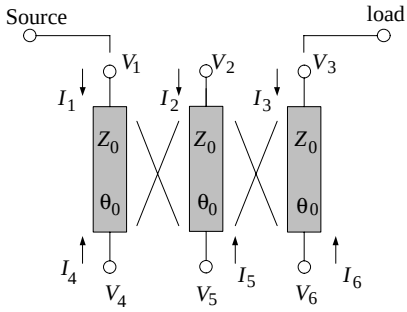

Figure 4. General equivalent circuit of the symmetric three-coupled-line structure.

the transmission zero T_{z4} in Figure 3(b) mainly determined by the short uniform resonator is located at $c/(4\sqrt{\varepsilon_e}d_2)$ GHz, whereas the transmission zero T_{z3} created by the short tapped stub basically keeps unchanged. Hence, the structures in Figures 1(c) and (e) may be applied to improve the sharp skirt and wide stopband performance of the microstrip filter.

2.2. Sharp Skirt and Wide Upper-stopband Broadband BPF with Two Different Size Tapped Stubs

The broadband BPF is designed by using symmetric three-coupled-line structure composed of a QWR side-coupled to two open stubs. Figure 4 depicts the general equivalent circuit of the structure with the termination conditions given by the following equations:

$$V_5 = 0; \quad I_2 = I_4 = I_6 = 0, \tag{2}$$

Thus, a simple analysis based on a transmission line model can be employed to investigate its filtering characteristics. As explained in [30], the parameters of three-coupled-line structure are completely obtained in terms of the static capacitance matrix with the dielectric in place and removed. Based on the analysis in [30, 31], the structure can produce three resonant modes, and the center frequency and passband bandwidth are mainly determined by the electrical length θ_0 of the QWR and the coupling gap, respectively.

To obtain a big 3 dB FBW, the BPF designed by using the structure with tight coupling in Figure 5(a) is simulated and optimized by HFSS. The simulated frequency responses in the range of 0.1–9 GHz are interpreted in Figure 5(b). The filter has three transmission zeros T_{z1}, T_{z2} and T_{z3} at the lower- and upper-stopbands, which are generated by the cross coupling between two open stubs and the

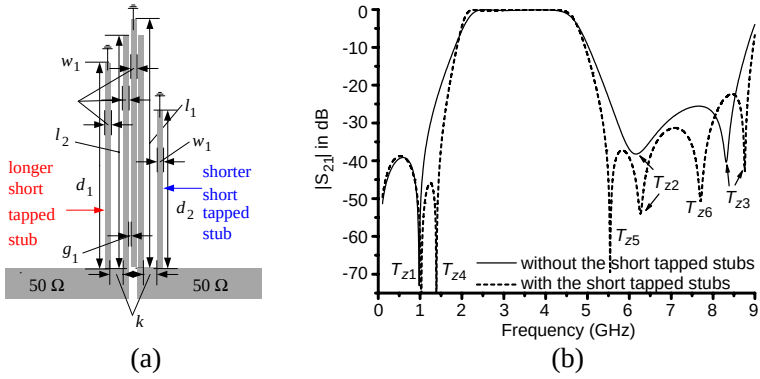

Figure 5. Schematic and frequency responses of the broadband BPFs with and without the different size short tapped stubs. (The structural parameters are: $l_1 = 16.7\,\text{mm}$; $l_2 = 16\,\text{mm}$; $d_1 = 15.2\,\text{mm}$; $d_2 = 10\,\text{mm}$; $w_1 = 0.3\,\text{mm}$; $g_1 = 0.1\,\text{mm}$; $k = 0.7\,\text{mm}$).

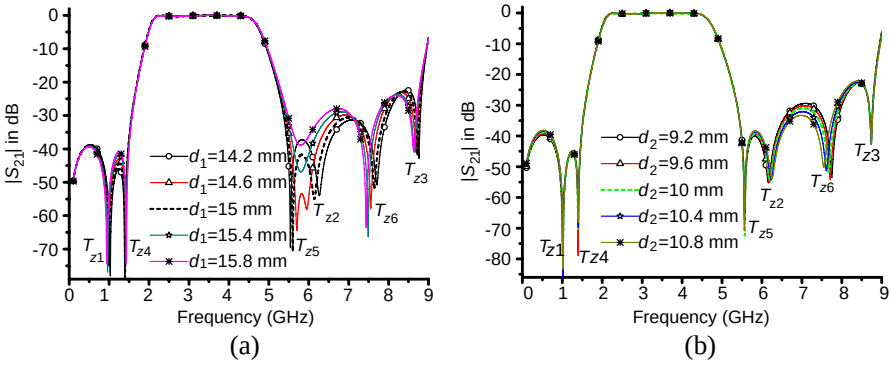

Figure 6. The simulated frequency responses. (a) With fixed $d_2 = 10\,\text{mm}$, varied d_1. (b) With fixed $d_1 = 14.5\,\text{mm}$, varied d_2.

coupling between the QWR and open stub [31]. In our previous work [32], the identical short stubs loaded in the 50 Ω feed lines of the broadband BPF with the dual-mode folded-T-type resonator can be applied to generate multiple transmission zeros. Here, the broadband BPF with the different size short tapped stubs in Figure 5(a) is simulated and the $|S_{21}|$ in dB is illustrated in Figure 5(b). We can see that three new transmission zeros T_{z4}, T_{z5} and T_{z6} can be created near the passband edge and in the upper-stopband. Further, Figures 6(a) and (b) give the frequency responses with varied lengths d_1 and d_2, respectively. As the length d_1 increased from 14.2 to 15.8 mm in

Figure 6(a), the transmission zeros T_{z1}, T_{z2}, T_{z3} and T_{z6}, specially the transmission zeros T_{z2} and T_{z6}, move towards the lower frequency, but the transmission zero T_{z5} near the passband edge shifts upwards. The transmission zeros in Figure 6(b) remain almost unchanged, except the T_{z6} moves towards the lower frequency, while changing the length d_2 from 9.2 to 10.8 mm. Thus, a compact broadband BPF can be realized with sharp skirt and deep stopband performance by simply adjusting the lengths d_1 and d_2.

2.3. Sharp Skirt and Wide Lower-stopband BPF with Tapped Stub

As shown in Figure 7(a), the BPF for WLAN application consists of two coupling QWRs, denoted by the length $l_1 + l_2 + l_3$ and width w_1, and short microstrip feedlines ($k_1 + k_2$, w_1). The passband frequency depends on the electrical length of the resonator. External quality factors and coupling coefficients are determined by the gap g_1 and the length k_2. The frequency responses with varied k_2 are simulated in the range of 0.1–11 GHz and interpreted in Figure 7(b). We can see that two transmission zeros T_{z1} and T_{z2} can be generated near the passband edge. As explained in [33], the short feedline can control source-load coupling easily to produce an equivalent feedback capacitor between I/O ports. Hence, the transmission zero T_{z2} created by the source-load coupling moves towards the passband edge, whereas the in-band and lower-stopband performance remain almost unchanged, as the length k_2 increased. But the length k_2 need to be reasonably

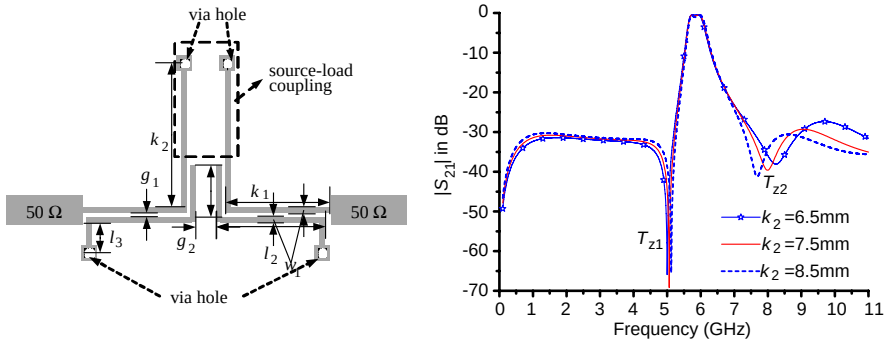

Figure 7. Schematic of the BPF in [33] and frequency responses with varied k_2. (The structural parameters are: $l_1 = 3.0$ mm; $l_2 = 5.0$ mm; $l_3 = 1.9$ mm; $k_1 = 5.0$ mm; $g_1 = 0.22$ mm; $g_2 = 0.8$ mm; $w_1 = 0.3$ mm).

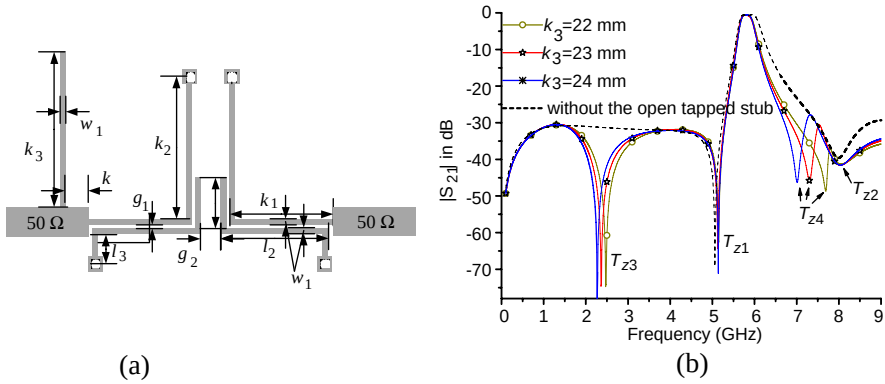

Figure 8. Schematic of the BPF with one open tapped stub and the frequency responses with varied k_3, fixed $k = 1.0$ mm.

chosen to obtain sharp skirt and compact size. Meanwhile, the filter with very deep lower-stopband performance can be realized, for the QWR has no resonate mode in lower-stopband.

Furthermore, the filter with one open stub with the length k_3 and width w_1 loaded in the 50 Ω feed line is simulated and compared in Figure 8. Two transmission zeros T_{z3} and T_{z4} created by the open tapped stub can be adjusted in the lower-stopband and near the upper passband edge, which sharpen the skirt and deepen the stopband. However, the center frequency shifts downwards and the bandwidth become narrower. So the length $l_1 + l_2 + l_3$ and the gaps g_1, g_2 need to be simply readjusted to obtain desired in-band performance.

2.4. High Isolation Microstrip Diplexer for Broadband and WLAN Application

Based on the features of the aforementioned sharp skirt and wide upper-stopband broadband BPF with two different size short tapped stub in Figure 5(a) and sharp skirt and wide lower-stopband BPF with open tapped stub in Figure 8(a), a microstrip diplexer, as shown in Figure 9, may be designed through the combination of two filters. As a filter part, the longer short tapped stub in Figure 5(a) and open tapped stub in Figure 8(a) are directly connected to common port without extra junction matching network, so more compact size can also be realized.

The mutual loading effect of two filters can be further investigated. The broadband filter with coupling short tapped stub and WLAN filter with coupling open tapped stub, as shown in Figure 10, are

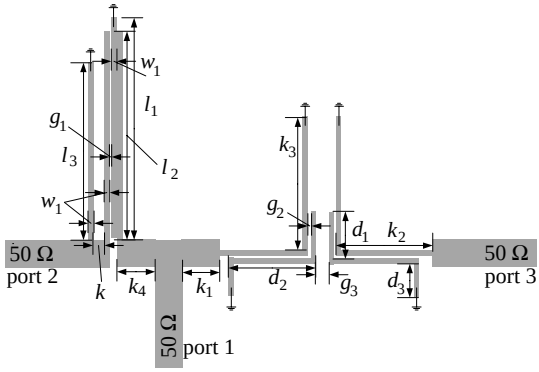

Figure 9. Schematic of the microstrip diplexer for GPS and WLAN application. (The structural parameters are: $l_1 = 16.7\,\text{mm}$; $l_2 = 16\,\text{mm}$; $l_3 = 10\,\text{mm}$; $w_1 = 0.3\,\text{mm}$; $d_1 = 3.0\,\text{mm}$; $d_2 = 5.0\,\text{mm}$; $d_3 = 1.9\,\text{mm}$; $k = 0.7\,\text{mm}$; $k_1 = k_4 = 2.22\,\text{mm}$; $k_2 = 5.0\,\text{mm}$; $k_3 = 7.5\,\text{mm}$; $g_1 = 0.1\,\text{mm}$; $g_2 = 0.22\,\text{mm}$; $g_3 = 0.8\,\text{mm}$).

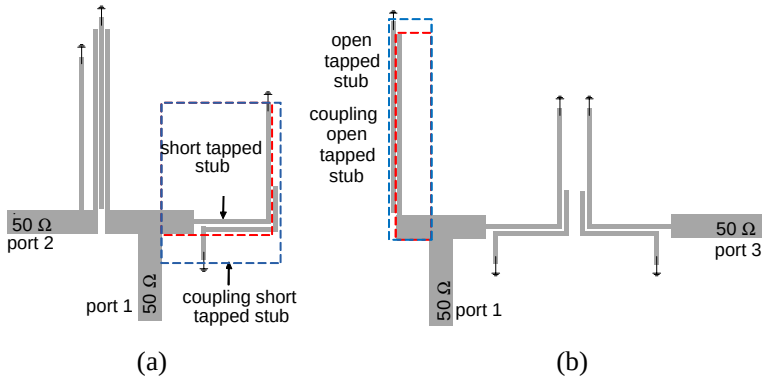

Figure 10. Configurations of the broadband filter with (a) the coupling short tapped stub and (b) the WLAN filter with the coupling open tapped stub.

simulated by HFSS, respectively. Figure 11 and Figure 12 give the simulated insertion losses of the broadband filter with coupling short tapped stub and WLAN filter with coupling open tapped stub. As discussed in Section 2.1, the QWRs in coupling short tapped stub and coupling open tapped stub can generate new transmission zeros T_{z7} and T_{z4}, respectively. Compared to the broadband filter with short tapped stub and WLAN filter with open tapped stub, only difference is that the transmission zeros T_{z2} and T_{z5}, near the transmission zero

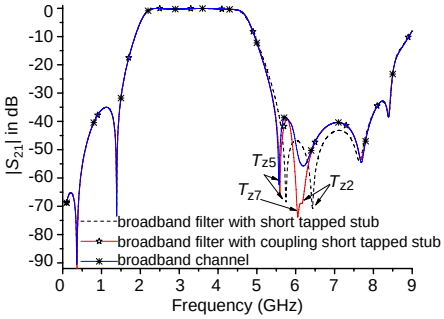

Figure 11. The $|S_{21}|$ in dB of the broadband filter with the coupling short tapped stub and broadband channel of the diplexer.

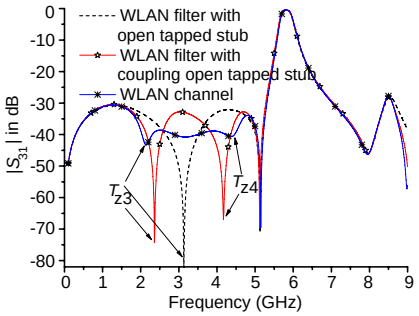

Figure 12. The $|S_{21}|$ in dB of the WLAN filter with the coupling open tapped stub and WLAN channel of the diplexer.

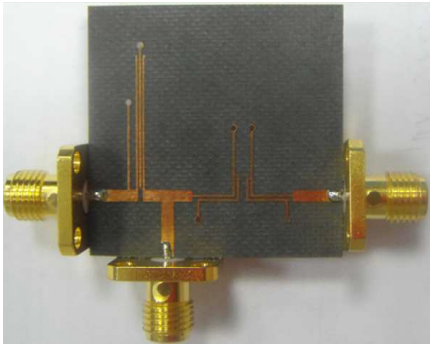

Figure 13. Photograph of the implemented proposed microstrip diplexer.

T_{z7}, and the transmission zero T_{z3}, near the transmission zero T_{z4}, are readjusted. Meanwhile, we can see from the Figure 11 and Figure 12 that the insertion losses of the broadband filter with coupling short tapped stub and WLAN filter with coupling open tapped stub show a better agreement with the corresponding channel in the diplexer. So, the mutual loading effect approximately equivalent to a coupled QWR can generate one new transmission zero at the passband edge to improve the isolation. Meanwhile, the compact diplexer remains the low insertion loss and high selective characteristics of two filters. To validate the design approach, the diplexer with 3 dB FBWs of 80% at 3.0 GHz for broadband channel and 5% at 5.8 GHz for WLAN channel is simulation and optimization by HFSS, and the dimensions are listed in Figure 9.

3. EXPERIMENTAL RESULTS

After studying the characteristics of the microstrip diplexer for broadband and WLAN application, the diplexer is fabricated on the Duroid 5880 substrate and its photogragh is shown in Figure 13. The filtering performance is measured by Agilent network analyzer N5230A. The simulated and measured frequency responses are shown in Figure 14, and illustrated good agreement. The losses and the slight shift in the center frequencies are attributed to manufacturing tolerances. The measured 3 dB FBWs are 80.3% at 3 GHz for broadband channel and 3.45% at 5.8 GHz for WLAN channel, with measured minimum insertion losses are −3 dB and the passband return loss better than −10.3 dB. Two transmission zeros near the broadband passband edge are located at 1.38 GHz and 5.65 GHz resulting in

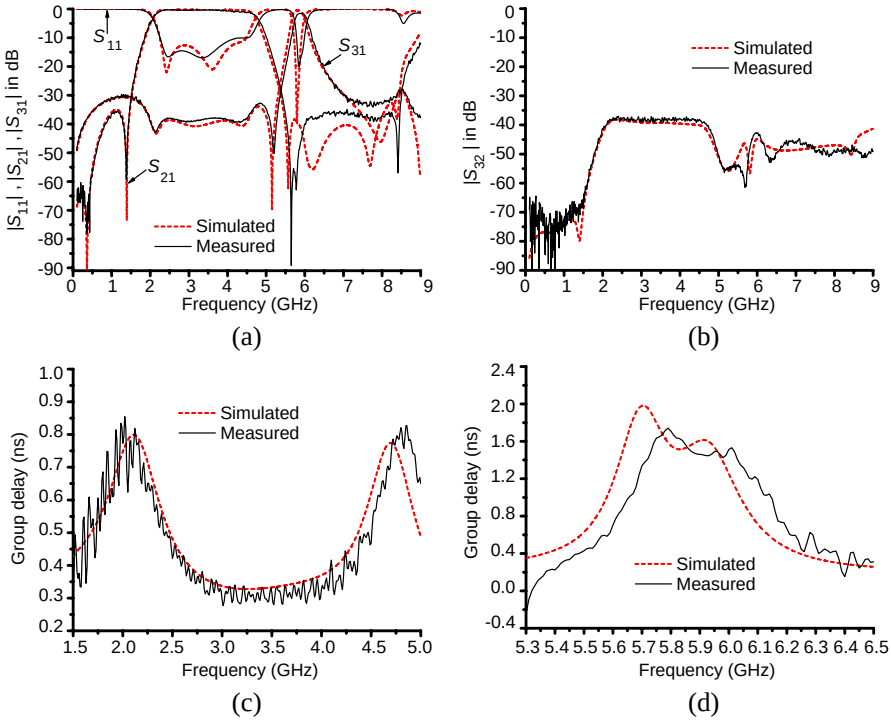

Figure 14. The simulated and measured frequency responses of the microstrip diplexer. (a) $|S_{11}|$, $|S_{21}|$, $|S_{31}|$ in dB. (b) $|S_{32}|$ in dB. (c) Group delay of the broadband channel. (d) Group delay of the WLAN channel.

sharp skirt, with an attenuation level of more than 59 dB. The upper-stopband of the broadband channel in experiment is extended up to 8.68 GHz with an insertion loss larger than 35 dB. The out-of-band rejection level of the WLAN channel is better than 30 dB in the range of 0.1–5.36 GHz and 7.01–9 GHz. Meanwhile, the measured isolation greater than 37.5 dB in broadband passband and more than 46 dB in WLAN passband, as shown in Figure 14(b), is achieved between two channels. In addition, the measured in-band group delay for broadband channel and WLAN channel in Figure 14(c) and Figure 14(d) vary from 0.3 to 0.6 ns and from 1.45 to 1.75 ns, respectively, which is quite small and flat in the broadband and WLAN passbands. The size without the 50 Ω feed lines is only $0.266\lambda \times 0.277\lambda$ in which λ is the guided wavelength at 3 GHz.

4. CONCLUSION

In this paper, a novel compact, low insertion loss, sharp skirt and high isolation microstrip diplexer for broadband and WLAN application is proposed through the combination of two out-band rejection BPFs with the tapped stub without the extra junction matching network. Due to the intrinsic characteristics and mutual loading effect of two filters, multiple transmission zeros can be generated to achieve sharp skirt, deep stopband and high isolation of the diplexer. Finally, a microstrip diplexer with the 3 dB FBWs of 80% at 3 GHz for broadband channel and 5% at 5.8 GHz for WLAN channel is designed and fabricated. The good agreement between the simulated and measured results demonstrates the validity of our proposed structure.

ACKNOWLEDGMENT

This work was supported by the Priority Academic Program Development of Jiangsu Higher Education Institutions (PAPD), Funding of Jiangsu Innovation Program for Graduate Education (No. CX10B_109Z) and Funding for Outstanding Doctoral Dissertation in NUAA (No. BCXJ10-06).

REFERENCES

1. Pozar, D. M., *Microwave Engineering*, Wiley, New York, 1998.
2. Matthaei, G. and E. G. Cristal, "Multiplexer channel-separating units using interdigital and parallel-coupled filters," *IEEE Transactions on Microwave Theory and Techniques*, Vol. 13, 328–334, 1965.

3. Wenzel, R. J., "Printed-circuit complementary filters for narrow bandwidth multiplexers," *IEEE Transactions on Microwave Theory and Techniques*, Vol. 16, 147–157, 1968.
4. Wang, R., J. Xu, M. Y. Wang, and Y. L. Dong, "Synthesis of microstrip resonator diplexers using linear frequency transformation and optimization," *Progress In Electromagnetics Research*, Vol. 124, 441–455, 2012.
5. Yang, T., P. L. Chi, and T. Itoh, "High isolation and compact diplexer using the hybrid resonators," *IEEE Microstrip and Wireless Components Letters*, Vol. 20, No. 10, 551–553, 2010.
6. Huang, C. Y., M. H. Weng, C. S. Ye, and Y. X. Xu, "A high band isolation and wide stopband diplexer using dual-mode stepped-impedance resonators," *Progress In Electromagnetics Research*, Vol. 100, 299–308, 2010.
7. Yang, R. Y., C. M. Hsiung, C. Y. Hung, and C. C. Lin, "Design of a high band isolation diplexer for GPS and WLAN system using modified stepped-impedance resonators," *Progress In Electromagnetics Research*, Vol. 107, 101–114, 2010.
8. Shi, J., J. X. Chen, and Z. H. Bao, "Diplexers based on microstrip line resonators with loaded elements," *Progress In Electromagnetics Research*, Vol. 115, 423–439, 2011.
9. Zeng, H. Y., G. M. Wang, D. Z. Wei, and Y. W. Wang, "Planar diplexer using composite right-/left-handed transmission line under balanced condition," *Electronics Letters*, Vol. 48, No. 2, 104–106, 2012.
10. Lin, Y.-L., S.-W. Lan, R.-Y. Yang, and C.-Y. Hung, "Design of a high band-isolation diplexer based on asymmetric stepped-impedance resonators with side-coupling structure," *Journal of Electromagnetic Waves and Applications*, Vol. 27, No. 1, 1–11, 2012.
11. Chen, C.-Y. and C.-C. Lin, "The design and fabrication of a highly compact microstrip dual-band bandpass filter," *Progress In Electromagnetics Research*, Vol. 112, 299–307, 2011.
12. Rezaee, P., M. Tayarani, and R. Knöchel, "Active learning method for the determination of coupling factor and external Q in microstrip filter design," *Progress In Electromagnetics Research*, Vol. 120, 459–479, 2011.
13. Chen, C. F., T. Y. Huang, C. P. Chou, and R. B. Wu, "Microstrip diplexers design with common resonator sections for compact size, but high isolation," *IEEE Transactions on Microwave Theory and Techniques*, Vol. 54, No. 5, 1945–1952, 2006.

14. Yang, T. P., L. Chi, and T. Itoh, "Compact quarter-wave resonator and its applications to miniaturized diplexer and triplexer," *IEEE Transactions on Microwave Theory and Techniques*, Vol. 59, No. 2, 260–269, 2011.
15. Chuang, M. L. and M. T. Wu, "Microstrip diplexer design using common T-shaped resonator," *IEEE Microwave and Wireless Components Letters*, Vol. 21, No. 11, 583–585, 2011.
16. Chen, C.-F., "Miniaturized and high isolation microstrip diplexers based on the tri-mode stubloaded stepped-impedance resonators," *Journal of Electromagnetic Waves and Applications*, Vol. 26, Nos. 14–15, 2001–2011, 2012.
17. Garcia-Lamperez, A., M. Salazar-Palma, and T. K. Sarkar, "Analytical synthesis of microwave multiport networks," *IEEE MTT-S Int. Microwave Symp. Digest*, 455–458, 2004.
18. Skaik, T. F., M. J. Lancaster, and F. Huang, "Synthesis of multiple output coupled resonator circuits using coupling matrix optimisation," *IET Microwaves, Antennas and Propagation*, Vol. 5, No. 9, 1081–1088, 2011.
19. Skaik, T. F. and M. J. Lancaster, "Coupled resonator diplexer without external junctions," *Journal of Electromagnetic Analysis and Applications*, Vol. 3, No. 6, 238–241, 2011.
20. An, J., G. M. Wang, C. X. Zhang, and P. Zhang, "Diplexer using composite right-/left-handed transmission line," *Electronics Letters*, Vol. 44, No. 11, 685–687, 2008.
21. Dong, Y. D. and T. Itoh, "Substrate integrated waveguide loaded by complementary split-ring resonators for miniaturized diplexer design," *IEEE Microwave and Wireless Components Letters*, Vol. 21, No. 1, 10–12, 2011.
22. Quan, X. L., R.-L. Li, J. Y. Wang, and Y. H. Cui, "Development of a broadband horizontally polarized omnidirectional planar antenna and its array for base stations," *Progress In Electromagnetics Research*, Vol. 128, 441–456, 2012.
23. Islam, M. T., R. Azim, and A. T. Mobashsher, "Triple band-notched planar UWB antenna using parasitic strips," *Progress In Electromagnetics Research*, Vol. 129, 161–179, 2012.
24. Russo, I., L. Boccia, G. Amendola, and H. Schumacher, "Compact hybrid coaxial architecture for 3-10 GHz UWB quasi-optical power combiners," *Progress In Electromagnetics Research*, Vol. 122, 77–92, 2012.
25. Azim, R. and M. T. Islam, "Compact planar UWB antenna with band notch characteristics for WLAN and DSRC," *Progress In*

Electromagnetics Research, Vol. 133, 391–406, 2013.

26. Ye, C. S., Y. K. Su, M. H. Weng, and C. Y. Hung, "A microstrip ring-like diplexer for bluetooth and UWB application," *Microwave and Optical Technology Letters*, Vol. 51, No. 6, 1518–1520, 2009.
27. Weng, M. H., C. Y. Hung, and Y. K. Su, "A hairpin line diplexer for direct sequence ultra-wideband wireless communications," *IEEE Microwave and Wireless Components Letters*, Vol. 17, No. 7, 519–521, 2007.
28. Ma, D., Z. Y. Xiao, L. Xiang, X. Wu, C. Huang, and X. Kou, "Compact dual-band bandpass filter using folded SIR with two stubs for WLAN," *Progress In Electromagnetics Research*, Vol. 117, 357–364, 2011.
29. Panda J. R. and R. S. Kshetrimayum, "A printed 2.4 GHz/5.8 GHz dual-band monopole antenna with a protruding stub in the ground plane for WLAN and RFID applications," *Progress In Electromagnetics Research*, Vol. 117, 425–434, 2011.
30. Nguyen, C. and K. Chang, "On the analysis and design of spurline band-stop filters," *IEEE Transactions on Microwave Theory and Techniques*, Vol. 33, No. 12, 1416–1421, 1985.
31. Song, K. and Q. Xue, "Novel broadband bandpass filters using Y-shaped dual-mode microstrip resonators," *IEEE Microwave and Wireless Components Letters*, Vol. 19, No. 9, 548–550, 2009.
32. Deng, H. W., Y. J. Zhao, X. S. Zhang, W. Chen, and L. Qiang, "Compact and high selectivity broadband bandpass filter with dual-mode folded-T-type resonator," *Microwave and Optical Technology Letters*, Vol. 53, No. 8, 1697–1700, 2011.
33. Dai, G. L., Y. X. Guo, and M. Y. Xia, "Design of compact bandpass filter with improved selectivity using source-load coupling," *Electronics Letters*, Vol. 46, No. 7, 505–506, 2010.